

Solution of periodic notch problems in an infinite plate using BIE in conjunction with remainder estimation technique

Y.Z. Chen*

Division of Engineering Mechanics, Jiangsu University, Zhenjiang, Jiangsu, 212013, P.R. China

(Received June 7, 2010, Accepted January 19, 2011)

Abstract. This paper provides a complex variable BIE for solving the periodic notch problems in plane plasticity. There is no limitation for the configuration of notches. For the periodic notch problem, the remainder estimation technique is suggested. In the technique, the influences on the central notch from many neighboring notches are evaluated exactly. The influences on the central notch from many remote notches are approximated by one term with a multiplying factor. This technique provides an effective way to solve the problems of periodic structures. Several numerical examples are presented, and most of them have not been reported previously.

Keywords: complex variable BIE; periodic notch problem; remainder estimation technique; stress concentration.

1. Introduction

When notches weaken a perfect tension plate, the hoop stress along the contour of notches will elevate significantly. This is so called the phenomena of stress concentration. Most researchers devoted their efforts to solve multiple circular hole problems, including the periodic circular hole problem (Horii and Nemat-Nassar 1985, Isida and Igawa 1991, Tsukrov and Kachanov 1997, Ting *et al.* 1999, Chen 1985, Wang *et al.* 2003, Chen and Lin 2007). Clearly, the suggested methods were limited to the circular configuration of hole only. For example, after the traction along the circular boundary of hole was expanded into a Fourier series, the multiple circular hole problem can be reduced to an algebraic equation for the undetermined Fourier coefficients (Horii and Nemat-Nassar 1985). For another example, a hypersingular integral equation was suggested to solve the addressed problem (Wang *et al.* 2003). In order to solve the hypersingular integral equation, the unknown displacement on the circular boundary was expanded into truncated complex Fourier series. Thus, the solution is only valid for the multiple circular hole problem. Therefore, those works have not provided a solution for multiple notches with arbitrary configuration, particularly, for the periodic notches.

The null-field integral equation for an infinite medium containing circular holes and/or inclusions

*Corresponding author, Professor, E-mail: chens@ujs.edu.cn

was developed (Chen and Wu 2007). The null-field integral equation was developed to analyze the stress state for a medium containing circular cavities under remote shear and two classical elasticity problems (Chen *et al.* 2006, 2010).

It is well known that the boundary integral equation (BIE) provides a general method to solve the boundary value problem of elasticity (Rizzo 1967, Cruse 1989, Jaswon and Symm 1967, Cheng and Cheng 2005, Brebbia *et al.* 1984, Hong and Chen 1988, Hromadka 1987, Linkov 2002, Chen and Chen 2004). A Review of dual boundary element methods was carried out in an earlier time (Chen and Hong 1999).

However, if one uses the BIE directly to solve the periodic notch problem, one may meet an inconvenient point. It is seen that the governing equation is generally formulated on the central notch, and the influences of infinite neighboring notches, from $-\infty$ -th, ..., -2-th, -1-th, 1st, 2nd, ∞ -th, must be evaluated exactly. In this case, one has to truncate sufficient terms to get a reasonable result. However, it is not easy to determine how many terms should be truncated in computation.

In this paper, a BIE is derived for solving the periodic notch problems, and the BIE is represented in the complex variable form. In the present study, there is no limitation for the configuration of notches. For the periodic notch problem, the remainder estimation technique is suggested. In the technique, the influences on the central notch from $-N$ -th, .. -2-th, -1-th, 1st, 2nd, ... N -th notches are evaluated exactly. In addition, the influences on the central notch from $-\infty$ -th, ..., $-(N+1)$ -th, $(N+1)$ -th, ... ∞ -th notches, are approximated by one term. This term is derived from the influences on the central notch from $-(N+1)$ -th and $(N+1)$ -th notches with a multiplying factor. This technique provides an effective way for the periodic notch problems. Several numerical examples are presented.

2. Formulation of BIE for periodic notch problems and the remainder estimation technique

Recently, the following boundary integral equation (BIE) for the exterior boundary value problem was suggested (Chen *et al.* 2009)

$$\frac{1}{2}u_i(\xi) + \int_{\Gamma} P_{ij}^*(\xi, x)u_j(x)ds(x) = \int_{\Gamma} U_{ij}^*(\xi, x)p_j(x)ds(x) \quad (i = 1, 2, \xi \in \Gamma) \quad (1)$$

where Γ is the contour of notch, and the kernel $P_{ij}^*(\xi, x)$ is defined by (Brebbia *et al.* 1984)

$$P_{ij}^*(\xi, x) = -\frac{1}{4\pi(1-\nu)r} \frac{1}{r} \{ (r_{,1}n_1 + r_{,2}n_2) ((1-2\nu)\delta_{ij} + 2r_{,i}r_{,j}) + (1-2\nu)(n_i r_{,j} - n_j r_{,i}) \} \quad (2)$$

where Kronecker deltas δ_{ij} is defined as, $\delta_{ij} = 1$ for $i = j$, $\delta_{ij} = 0$ for $i \neq j$, and

$$r_{,1} = \frac{x_1 - \xi_1}{r} = \cos \alpha, \quad r_{,2} = \frac{x_2 - \xi_2}{r} = \sin \alpha, \quad n_1 = -\sin \beta, \quad n_2 = \cos \beta \quad (3)$$

where the angles " α " and " β " are indicated in Fig. 1(a).

In the meantime, the kernel $U_{ij}^*(\xi, x)$ is defined by

$$U_{ij}^*(\xi, x) = \frac{1}{8\pi(1-\nu)G} \{ -(3-4\nu)\ln(r)\delta_{ij} + r_{,i}r_{,j} - 0.5\delta_{ij} \} \quad (4)$$

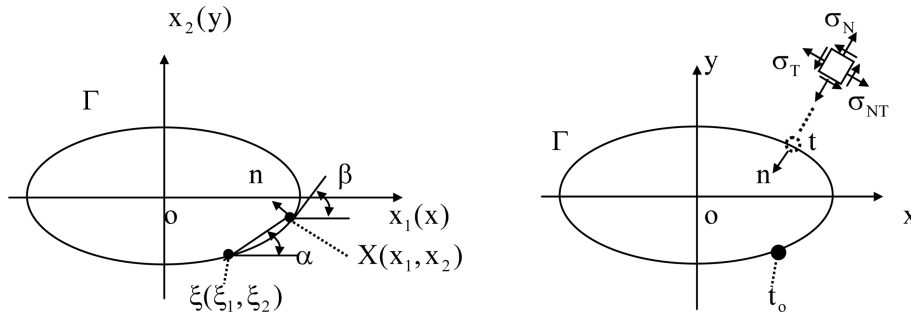


Fig. 1 (a) An elliptical notch in an infinite plate, (b) an elliptical notch in an infinite plate with notations for the formulation of complex variable BIE

It was noted that the kernel $U_{ij}^*(\xi, x)$ differed by a constant term $(-\delta_{ij}/16\pi(1-\nu)G)$ with the usual kernel in the textbook (Brebbia *et al.* 1984). The usual kernel for $U_{ij}^*(\xi, x)$ in available textbook can only be used for the case that the loadings on the contour are in equilibrium. It is emphasized here that the BIE shown by Eq. (1) can be used to the case of arbitrary loading even the applied loadings on the contour are not in equilibrium (Chen *et al.* 2009).

After using the Betti’s reciprocal theorem, or the Somigliana identity, between the fundamental stress field from the singular solution and the physical stress field, a complex variable BIE can be formulated (Chen *et al.* 2009, 2010, Muskhelishvili 1953). After some manipulations, the suggested complex variable BIE for plane elasticity is as follows (Fig. 1(b))

$$\begin{aligned} \frac{U(t_0)}{2} + B_1 i \int_{\Gamma} \left(-\frac{\kappa-1}{t-t_0} U(t) dt + L_1(t, t_0) U(t) dt - L_2(t, t_0) \overline{U(t)} dt \right) \\ = B_2 i \sum_{j=1}^N \int_{\Gamma} \left(-2\kappa \ln|t-t_0| Q(t) dt - \frac{t-t_0}{\bar{t}-\bar{t}_0} \overline{Q(t)} d\bar{t} \right) \end{aligned} \quad (5)$$

where

$$U(t) = u(t) + iv(t), \quad Q(t) = \sigma_N(t) + i\sigma_{NT}(t), \quad (t \in \Gamma) \quad (6)$$

$$B_1 = \frac{1}{2\pi(\kappa+1)}, \quad B_2 = \frac{1}{4\pi G(\kappa+1)} \quad (7)$$

$$L_1(t, \tau) = -\frac{d}{dt} \left\{ \ln \frac{t-\tau}{\bar{t}-\bar{\tau}} \right\} = -\frac{1}{t-\tau} + \frac{1}{\bar{t}-\bar{\tau}} \frac{d\bar{t}}{dt}$$

$$L_2(t, \tau) = \frac{d}{dt} \left\{ \frac{t-\tau}{\bar{t}-\bar{\tau}} \right\} = \frac{1}{\bar{t}-\bar{\tau}} - \frac{t-\tau}{(\bar{t}-\bar{\tau})^2} \frac{d\bar{t}}{dt} \quad (8)$$

In Eq. (6), $u(t) + iv(t)$ is the displacement, and $\sigma_N(t) + i\sigma_{NT}(t)$ is the traction applied along the contour of notch (Fig. 1(b)). In Eq. (7), G is shear modulus of elasticity, $\kappa = (3-4\nu)$ in plane strain case, $\kappa = (3+\nu)/(1-\nu)$ in plane stress case, and ν is the Poisson’s ratio.

It is found that two types of representation shown by Eqs. (1) and (5) are equivalent (Chen *et al.* 2009, 2010). However, the representation of Eq. (5) has some advantages. For example, the

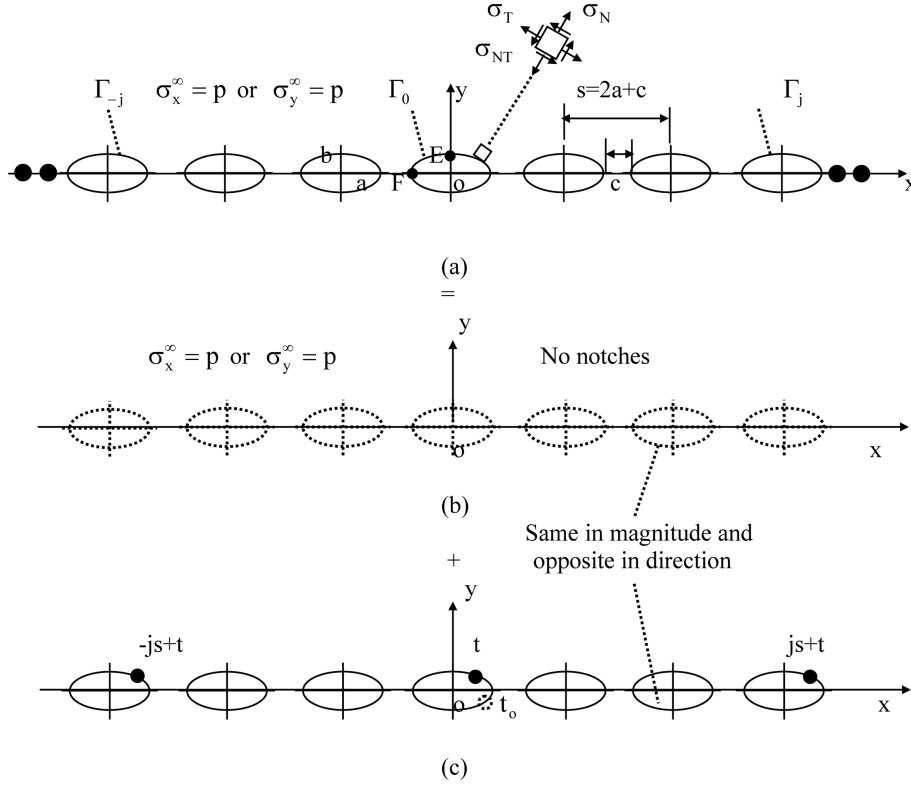


Fig. 2 Periodic elliptical notches with remote loading $\sigma_x^\infty = p$ or $\sigma_y^\infty = p$, (a) the original problem, (b) the uniform field, (c) the perturbation field

property of the kernels in the BIE is clearly indicated. It is seen from Eq. (5) that the term $U(t)dt/(t-t_0)$ is a Cauchy principle value integral, and two terms $L_1(t, t_0)U(t)dt$ and $L_2(t, t_0)U(t)dt$ are regular integral.

The periodic notch problem in an infinite plate is indicated in Fig. 2. The original field shown by Fig. 2(a) can be considered as a superposition of the uniform field and the perturbation field shown by Fig. 2(b) and 2(c), respectively. Clearly, we only need to solve the problem for the perturbation field shown by Fig. 2(c). Since the problem has a periodic property, the BIE can be formulated on the 0-th (the central one) notch. From Eq. (5), we have the following BIE

$$\begin{aligned} & \frac{U(t_0)}{2} + B_1 i \sum_{j=-\infty}^{\infty} \int_{\Gamma_j} \left(-\frac{\kappa-1}{t-t_0} U(t)dt + L_1(t, t_0)U(t)dt - L_2(t, t_0)\overline{U(t)dt} \right) \\ & = B_2 i \sum_{j=-\infty}^{\infty} \int_{\Gamma_j} \left(-2\kappa \ln|t-t_0|Q(t)dt - \frac{t-t_0}{\bar{t}-\bar{t}_0}\overline{Q(t)d\bar{t}} \right) \quad (t_0 \in \Gamma_0) \end{aligned} \tag{9}$$

The remainder estimation technique is introduced below. After discretization, the BIE (9) can be written in the form

$$\frac{U(t_0)}{2} + \sum_{j=-\infty}^{\infty} \mathbf{M}_{U,j} \mathbf{U} = \sum_{j=-\infty}^{\infty} \mathbf{M}_{Q,j} \mathbf{Q} \quad (t_0 \in \Gamma_0) \tag{10}$$

where “**U**” and “**Q**” denote vector for the displacement (for $U(t) = u(t) + iv(t)$) and traction (for $Q(t) = \sigma_N(t) + i\sigma_{NT}(t)$) on the notch contour, respectively. In Eq. (10), $\mathbf{M}_{U,j}$ and $\mathbf{M}_{Q,j}$ represent the relevant influence matrix from the j -th notch to the 0-th notch (the central notch Γ_o) (Fig. 2). From Eq. (10) we see that we must perform superposition of the matrix $\mathbf{M}_{U,j}$ and $\mathbf{M}_{Q,j}$ from $j = -\infty, \dots, -2, -1, 0, 1, 2, \dots$ to $j = \infty$. In the approximate computation, one may truncate finite terms in the summation, for example, from $j = -N, \dots, -2, -1, 0, 1, 2, \dots$ to $j = N$. However, it is not easy to get sufficient accurate result from the assumed approximation. In order to overcome this difficulty, the remainder estimation technique is suggested below.

For the approximation of $\sum_{j=-\infty}^{\infty} \mathbf{M}_{U,j}$, the remainder estimation technique was suggested (Chen *et al.* 2008). Now we study the approximation for the summation $\sum_{j=-\infty}^{\infty} \mathbf{M}_{Q,j}$.

As a typical term, we take the following integral in right hand side of Eq. (9), which is as follows

$$H_j = \int_{\Gamma_{-j}} \ln|t-t_o|Q(t)dt + \int_{\Gamma_j} \ln|t-t_o|Q(t)dt \quad (t_o \in \Gamma_o) \tag{11}$$

Physically, the integral H_j represents the summation of influences of $-j$ -notch and j -th notch to the 0-th notch (the central notch Γ_o). Note that, in Eq. (11), $t_o \in \Gamma_o$, and $t \in \Gamma_{-j}$ or $t \in \Gamma_j$. Secondly, in the periodic problem, $Q(t)$ is the same function for all notches. Thus, the integral (11) can be rewritten as (Fig. 2(c))

$$H_j = \int_{\Gamma_o} \ln|js-(t-t_o)|Q(t)dt + \int_{\Gamma_o} \ln|js+(t-t_o)|Q(t)dt \quad (t_o \in \Gamma_o) \tag{12}$$

Note that, in Eq. (11) the “ dt ” is along Γ_{-j} or Γ_j . However, in Eq. (12) “ dt ” is along Γ_o .

Clearly, in the perturbation field shown by Fig. 2(c), the traction on the individual notch contour is in equilibrium. Thus, we have

$$\int_{\Gamma_j} Q(t)dt = 0, \quad (j = -\infty, -2, -1, 0, 1, 2, \dots \text{ to } j = \infty) \tag{13}$$

After using the condition (13), we find

$$H_j \approx \frac{1}{(js)^2} \int_{\Gamma_o} 2(c^2 + d^2)Q(t)dt, \quad \text{with } c = \text{Re}|t-t_o|, \quad d = \text{Im}|t-t_o|$$

$$(t_o \in \Gamma_o, \text{ for sufficient large } j) \tag{14}$$

In Eq. (14), “ s ” ($s = 2a + c$) denotes a distance between two notches (Fig. 2). Similarly, we have

$$H_{N+1} \approx \frac{1}{((N+1)s)^2} \int_{\Gamma_o} 2(c^2 + d^2)Q(t)dt$$

$$(t_o \in \Gamma_o, \text{ for sufficient large } N + 1) \tag{15}$$

From Eqs. (14) and (15), the following approximation is found

$$H_j \approx \frac{(N+1)^2}{j^2} H_{N+1}$$

$$(t_o \in \Gamma_o, \text{ for sufficient large } j \text{ and } N + 1) \tag{16}$$

In addition, from Eq. (16), we have

$$\sum_{j=N+1}^{\infty} H_j \approx (N+1)^2 H_{N+1} \sum_{j=N+1}^{\infty} \frac{1}{j^2} = \gamma H_{N+1} \quad (17)$$

where

$$\gamma = (N+1)^2 \sum_{j=N+1}^{\infty} \frac{1}{j^2} = (N+1)^2 \left(\frac{\pi^2}{6} - \sum_{j=1}^N \frac{1}{j^2} \right) \quad (18)$$

Eq. (17) means that the influences from many remote notches ($j = -\infty, \dots, j = -(N+1)$, $j = N+1, \dots$ to $j = \infty$) can be approximated by one term H_{N+1} with a multiplying factor γ . It is seen that two integrals in the right side of Eq. (9) have the same property as indicated by Eq. (17). Thus, we have

$$\begin{aligned} \sum_{j=-\infty}^{\infty} \mathbf{M}_{Q,j} &= \mathbf{M}_{Q,0} + \sum_{j=1}^N (\mathbf{N}_{Q,-j} + \mathbf{M}_{Q,j}) + \sum_{j=N+1}^{\infty} (\mathbf{M}_{Q,-j} + \mathbf{M}_{Q,j}) \\ &\approx \mathbf{M}_{Q,0} + \sum_{j=1}^N (\mathbf{N}_{Q,-j} + \mathbf{M}_{Q,j}) + \gamma (\mathbf{M}_{Q,-(N+1)} + \mathbf{M}_{Q,N+1}) \end{aligned} \quad (19)$$

Eq. (19) means that the infinite summation $\sum_{j=N+1}^{\infty} (\mathbf{M}_{Q,-j} + \mathbf{M}_{Q,j})$ is approximated by one term $\gamma (\mathbf{M}_{Q,-(N+1)} + \mathbf{M}_{Q,N+1})$. This technique is called the remainder estimation technique (Chen *et al.* 2008). From numerical example, we will see that this technique provides an effective way to the periodic notch problem.

Similarly, we can propose

$$\sum_{j=-\infty}^{\infty} \mathbf{M}_{U,j} \approx \mathbf{M}_{U,0} + \sum_{j=1}^N (\mathbf{M}_{U,-j} + \mathbf{M}_{U,j}) + \gamma (\mathbf{M}_{U,-(N+1)} + \mathbf{M}_{U,N+1}) \quad (20)$$

3. Numerical examples

The following numerical examples are devoted to examine the efficiency and accuracy of the suggested method. Most results in the numerical examples have not been reported previously. Some of them are compared with the known results.

3.1 Example 1

In the first example, the periodic elliptic notches are applied by remote tension $\sigma_x^\infty = p$ (Fig. 2). Clearly, after using the superposition principle, the original problem shown by Fig. 2(a) can be reduced to two problems shown by Fig. 2(b),(c). Thus, the main work is to solve the problem for the perturbation field, which is shown by Fig. 2(c). The elliptic notch has two axes “a” and “b” and the spacing between two notches is denoted by “c” (Fig. 2).

As claimed above, the remainder estimation technique is used in computation. In the computation, the following linear shape function for $U(s)$ (or $Q(s)$) on an interval $s \leq |d|$ is used

$$U(s) = f_1 \frac{d-s}{2d} + f_2 \frac{d+s}{2d}, \quad |s| \leq d \quad (\text{with } U(s)|_{s=-d} = f_1, \quad U(s)|_{s=d} = f_2) \quad (21)$$

$M = 180$ divisions for the elliptic contour are used in computation, and $N = 20$ is used in Eqs. (19) and (20).

For evaluating the hoop stress σ_T , the following technique is suggested. In fact, in the plane strain

Table 1 The non-dimensional hoop stress $f(f = \sigma_T/p)$ at points E and F on the elliptical notch under the remote loading $\sigma_x^o = p$ (see Eq. (23) and Fig. 2)

(1) $b/a = 0.5$ case, $c/a = 0.1, 0.2, \dots, 1$

$c/a =$	0.1	0.2	0.3	0.4	0.5	0.6	0.7	0.8	0.9	1
Points										
E	1.413	1.430	1.448	1.464	1.482	1.499	1.516	1.533	1.550	1.567
F	0.006	-0.005	-0.046	-0.105	-0.170	-0.231	-0.289	-0.342	-0.389	-0.431

(2) $b/a = 0.5$ case, $c/a = 1, 2, \dots, 10$

$c/a =$	1	2	3	4	5	6	7	8	9	10
Points										
E	1.567	1.703	1.792	1.848	1.885	1.910	1.928	1.941	1.951	1.958
F	-0.431	-0.687	-0.800	-0.861	-0.898	-0.921	-0.936	-0.947	-0.957	-0.963

(3) $b/a = 1$ case, $c/a = 0.1, 0.2, \dots, 1$

$c/a =$	0.1	0.2	0.3	0.4	0.5	0.6	0.7	0.8	0.9	1
Points										
E	1.702	1.728	1.753	1.777	1.802	1.827	1.851	1.874	1.897	1.920
F	0.005	0.003	0.003	0.003	-0.002	-0.013	-0.030	-0.053	-0.079	-0.108

(4) $b/a = 1$ case, $c/a = 1, 2, \dots, 10$

$c/a =$	1	2	3	4	5	6	7	8	9	10
Points										
E	1.920	2.139	2.325	2.470	2.579	2.659	2.720	2.767	2.803	2.831
F	-0.108	-0.385	-0.568	-0.684	-0.759	-0.810	-0.848	-0.875	-0.895	-0.911

(5) $b/a = 2$ case $c/a = 0.1, 0.2, \dots, 1$

$c/a =$	0.1	0.2	0.3	0.4	0.5	0.6	0.7	0.8	0.9	1
Points										
E	2.144	2.182	2.218	2.252	2.287	2.323	2.357	2.390	2.423	2.455
F	0.003	0.002	0.001	0.002	0.001	0.001	0.002	0.002	0.002	0.002

(6) $b/a = 2$ case, $c/a = 1, 2, \dots, 10$

$c/a =$	1	2	3	4	5	6	7	8	9	10
Points										
E	2.455	2.755	3.029	3.283	3.512	3.714	3.886	4.032	4.154	4.258
F	0.002	-0.068	-0.214	-0.355	-0.469	-0.559	-0.629	-0.686	-0.731	-0.768

case, we have the following relation

$$\sigma_T = \frac{E\varepsilon_T + \nu(1 + \nu)\sigma_N}{1 - \nu^2} \quad (22)$$

where E is the Young's modulus of elasticity, and ν the Poisson's ratio. In Eq. (22), the component σ_N is from input datum, and ε_T is the strain in the T -direction, which can be evaluated from the solution of displacement along the boundary. Thus, the values of σ_T at many discrete points can be evaluated.

The computed stress for σ_T is expressed as

$$\sigma_T = f(b/a, c/a)p \quad (23)$$

Under the conditions: (1) $b/a = 0.5, 1$ and 2 , (2) and $c/a = 0.1, 0.2, \dots, 1.0$, or $c/a = 1, 2, \dots, 10$, and (3) at the points "E" and "F" (Fig. 2), the computed results are listed in Table 1. From Table 1 we see that the interaction of two notches is significant. For example, for $c/a = 0.1$ case, we have $f(b/a, c/a) = 1.413, 1.702$ and 2.144 at the point "E" for $b/a = 0.5, 1$ and 2 , respectively. However, in the same condition of single notch case, we have $f = 2, 3$ and 5 at the point "E" for $b/a = 0.5, 1$ and 2 , respectively. In addition, in the condition of $b/a = 1$, the computed results are approximately same as obtained in other source (Wang *et al.* 2003).

3.2 Example 2

In the second example, the remote loading is $\sigma_y^\infty = p$ (Fig. 2). The other computation conditions are the same as in the first example. The stress for σ_T is also denoted by $\sigma_T = f(b/a, c/a)p$ shown by Eq. (23). The computed results are listed in Table 2. From the computed results we see that the stress state $\sigma_y^\infty = p$ has a significant influence to the stress distribution along contour.

For example, (1) for $c/a = 0.1$ case, we have $f(b/a, c/a) = 23.608, 21.693$ and 21.201 , (2) for $c/a = 1$ case, we have $f(b/a, c/a) = 6.178, 3.923$ and 3.231 at the point "F" for $b/a = 0.5, 1$ and 2 , respectively (Fig. 2). However, in the same condition of single notch case, we have $f = 5, 3$ and 2 at the point "F" for $b/a = 0.5, 1$ and 2 , respectively. In addition, in the condition of $b/a = 1$, the computed results are approximately same as obtained in other source (Wang *et al.* 2003).

In addition, comparison between different techniques is also made. For the case of $b/a = 1$ and $c/a = 0.1$, if choosing $N = 10$ and $N = 20$ in Eqs. (19) and (20), and using the remainder estimation technique, we have $f(b/a, c/a) = 21.700$ and 21.693 , respectively. That is to say, the number truncated is not sensitive to the final results. Note that, $N = 10$ is equivalent to $23 (= 2*(10 + 1) + 1)$ terms are truncated in Eqs. (19) and (20), and $N = 20$ is equivalent to $43 (= 2*(20 + 1) + 1)$ terms are truncated in Eqs. (19) and (20).

However, For the case of $b/a = 1$ and $c/a = 0.1$ in the other source of computation using different technique (Wang *et al.* 2003), computed results are $f(b/a, c/a) = 18.905, 20.276$ and 21.124 , for truncating $21, 41$ and 101 terms, respectively. That is to say, the number of truncated terms is sensitive to the final results, if the remainder estimation technique was not used.

3.3 Example 3

In the third example, the remote loading is $\sigma_y^\infty = p$. The other computation conditions are same as

Table 2 The non-dimensional hoop stress $f(f = \sigma_T/p)$ at points E and F on the elliptical notch under the remote loading $\sigma_y^\infty = p$ (see Eq. (23) and Fig. 2)

(1) $b/a = 0.5$ case, $c/a = 0.1, 0.2, \dots, 1$

$c/a =$	0.1	0.2	0.3	0.4	0.5	0.6	0.7	0.8	0.9	1
Points										
E	-0.670	-0.665	-0.660	-0.658	-0.659	-0.661	-0.665	-0.672	-0.678	-0.686
F	23.608	13.610	10.347	8.772	7.861	7.275	6.870	6.577	6.352	6.178

(2) $b/a = 0.5$ case, $c/a = 1, 2, \dots, 10$

$c/a =$	1	2	3	4	5	6	7	8	9	10
Points										
E	-0.686	-0.771	-0.837	-0.880	-0.908	-0.928	-0.941	-0.952	-0.960	-0.966
F	6.178	5.457	5.254	5.162	5.114	5.083	5.063	5.050	5.042	5.035

(3) $b/a = 1$ case, $c/a = 0.1, 0.2, \dots, 1$

$c/a =$	0.1	0.2	0.3	0.4	0.5	0.6	0.7	0.8	0.9	1
Points										
E*	-0.574	-0.570	-0.566	-0.562	-0.560	-0.559	-0.559	-0.559	-0.560	-0.562
E**	-0.570	-0.568	-0.564	-0.562	-0.560	-0.559	-0.558	-0.559	-0.560	-0.561
E#	-0.607	-0.592			-0.574					
F*	21.700	11.703	8.384	6.733	5.754	5.114	4.670	4.348	4.107	3.923
F**	21.693	11.701	8.382	6.732	5.753	5.114	4.669	4.348	4.107	3.923
F#	21.124	11.514			5.711					

(4) $b/a = 1$ case, $c/a = 1, 2, \dots, 10$

$c/a =$	1	2	3	4	5	6	7	8	9	10
Points										
E*	-0.562	-0.612	-0.682	-0.744	-0.794	-0.832	-0.861	-0.884	-0.902	-0.915
E**	-0.561	-0.611	-0.681	-0.744	-0.794	-0.832	-0.861	-0.884	-0.902	-0.915
E#	-0.571	-0.618			-0.687					
F*	3.923	3.240	3.095	3.045	3.024	3.014	3.008	3.005	3.003	3.002
F**	3.923	3.240	3.095	3.046	3.024	3.014	3.009	3.005	3.004	3.001
F#	3.910	3.237			3.094					

*truncating 23 terms and using the remainder estimation technique

**truncating 43 terms and using the remainder estimation technique

#truncating 101 terms and using hypersingular integral equation (Wang *et al.* 2003)

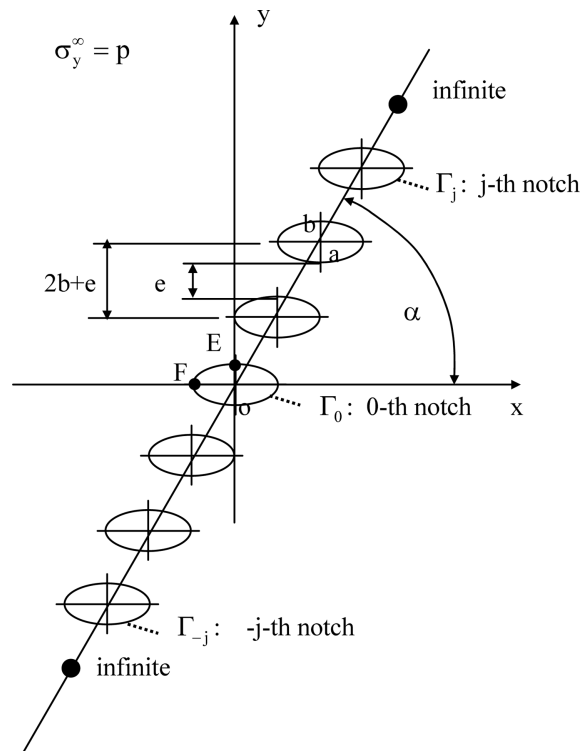
(5) $b/a = 2$ case, $c/a = 0.1, 0.2, \dots, 1$

$c/a =$	0.1	0.2	0.3	0.4	0.5	0.6	0.7	0.8	0.9	1
Points										
E	-0.482	-0.479	-0.477	-0.476	-0.474	-0.473	-0.472	-0.471	-0.471	-0.471
F	21.201	11.184	7.855	6.195	5.201	4.541	4.071	3.720	3.447	3.231

Table 2 Continued

(6) $b/a = 2$ case, $c/a = 1, 2, \dots, 10$

$c/a =$	1	2	3	4	5	6	7	8	9	10
Points										
E	-0.471	-0.481	-0.512	-0.555	-0.603	-0.651	-0.693	-0.731	-0.763	-0.791
F	3.231	2.318	2.095	2.020	1.992	1.981	1.977	1.977	1.978	1.979

Fig. 3 Periodic elliptical notches in an inclined position with remote loading $\sigma_y^\infty = p$

in the first example. The notches are arranged in an inclined position (Fig. 3). The vertical distance between two centers of neighboring notches is $s = 2b + e$, and the horizontal distance is $(2b + e)/\tan\alpha$ (Fig. 3).

The computed hoop stress σ_T is expressed as

$$\sigma_T = g(b/a, e/b, \alpha, \theta)p \quad (\text{for boundary points } x = a\cos\theta \quad y = b\sin\theta) \quad (24)$$

In the example, we choose: (1) $b/a = 0.5$, $b/a = 1$ and $b/a = 2$, (2) $e/b = 0.5$, (3) $\alpha = 2\pi/12$, $3\pi/12$, $4\pi/12$ and $5\pi/12$. The computed non-dimensional hoop stresses for three cases $b/a = 0.5$, $b/a = 1$ and $b/a = 2$ are plotted in Figs. 4, 5 and 6, respectively.

From the plotted results we see that the hoop stress distributions along the elliptical contour are very complicated, and the following results have been found:

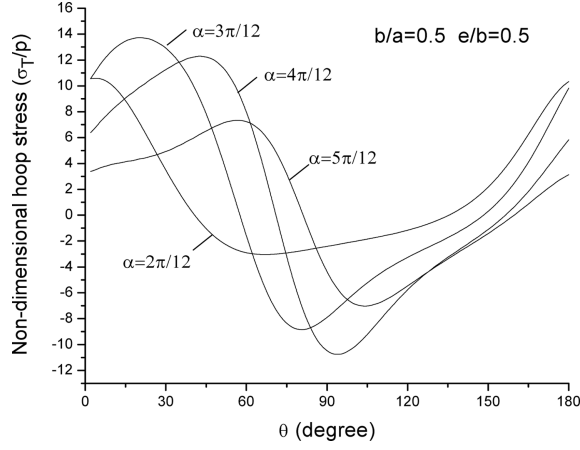


Fig. 4 The non-dimensional hoop stress $g(g(e/b, b/a, \alpha, \theta) = \sigma_T/p)$ at points $(x = a\cos\theta, y = b\sin\theta)$ along the elliptical notch under the remote loading σ_y^∞ in the case of $b/a = 0.5$ and $e/b = 0.5$ (see Eq. (24) and Fig. 3)

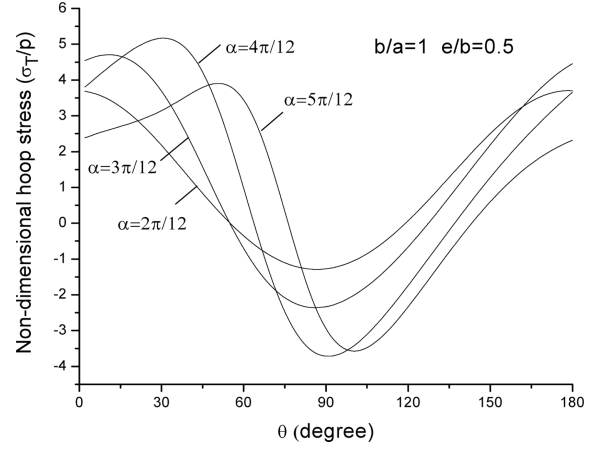


Fig. 5 The non-dimensional hoop stress $g(g(e/b, b/a, \alpha, \theta) = \sigma_T/p)$ at points $(x = a\cos\theta, y = b\sin\theta)$ along the elliptical notch under the remote loading σ_y^∞ in the case of $b/a = 1$ and $e/b = 0.5$ (see Eq. (24) and Fig. 3)

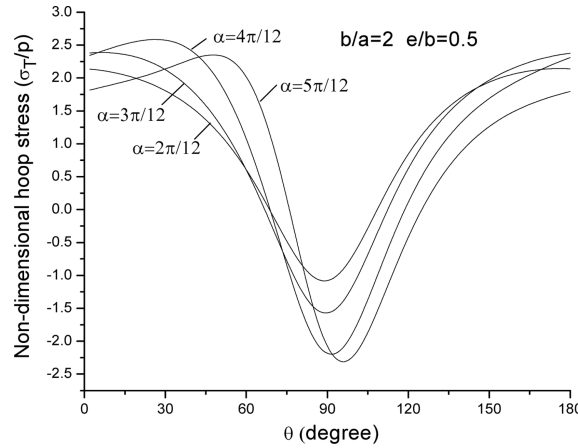


Fig. 6 The non-dimensional hoop stress $g(g(e/b, b/a, \alpha, \theta) = \sigma_T/p)$ at points $(x = a\cos\theta, y = b\sin\theta)$ along the elliptical notch under the remote loading in the case of $b/a = 2$ and $e/b = 0.5$ (see Eq. (24) and Fig. 3)

- (1) In the case of $b/a = 0.5$, $e/b = 0.5$ and $\alpha = \pi/4$, we have $g_{\max} = 13.759$ at $\theta = 20^\circ$, and $g_{\min} = -8.844$ at $\theta = 80^\circ$. We know that, we have $g_{\max} = 5$ and $g_{\min} = -1$, for the single notch case. In this case, the stress concentration factor reaches a rather high value.
- (2) In the case of $b/a = 1$, $e/b = 0.5$ and $\alpha = \pi/4$, we have $g_{\max} = 4.708$ at $\theta = 12^\circ$ and $g_{\min} = -2.361$ at $\theta = 86^\circ$. We know that, we have $g_{\max} = 3$ and $g_{\min} = -1$, for the single notch case.
- (3) In the case of $b/a = 2$, $e/b = 0.5$ and $\alpha = \pi/4$, we have $g_{\max} = 2.388$ at $\theta = 6^\circ$ and $g_{\min} = -1.573$ at $\theta = 90^\circ$. We know that, we have $g_{\max} = 2$ and $g_{\min} = -1$, for the single notch case.

4. Conclusions

The solution for the periodic notch problem is derived directly from a suggested BIE (9). Therefore, there is no limitation for the notch configuration. Secondly, the suggested remainder estimation technique provides an effective way for the periodic notch problem. For example, in the case of $b/a = 1$, $c/a = 0.1$ and $\sigma_y^\infty = p$ (Fig. 2), we have the non-dimensional maximum hoop stresses 21.700 and 21.693, for truncating 23 and 43 terms, respectively. In the meantime, the non-dimensional maximum hoop stresses by using other method are as follows: 18.905, 20.276 and 21.124, for truncating 21, 41 and 101 terms, respectively (Wang *et al.* 2003). Clearly, the efficiency of the remainder estimation technique can be seen from the comparison results.

Eq. (16) reveals that the influence caused by traction on the central notch from $-j$ -th and j -th notches is nearly proportional to or $1/j^2$. This character provides a solid basis in the analysis. Previously, the number of the truncated number is only determined by researcher's experience. However, if the suggested remainder estimation technique is used, a stable numerical result can be achieved. Since the situation of the elliptic notch is similar to case of circle hole, the remainder estimation technique can also provide an accurate result in the case of the elliptic periodic notch.

References

- Brebbia, C.A., Telles, J.C.F. and Wrobel, L.C. (1984), *Boundary Element Techniques – Theory and Applications in Engineering*, Springer, Heidelberg.
- Chen, J.T. and Hong, H.K. (1999), "Review of dual boundary element methods with emphasis on hypersingular integrals and divergent series", *ASME Appl. Mech. Rev.*, **52**, 17-33.
- Chen, J.T. and Chen, Y.W. (2004), "Dual boundary element analysis using complex variables for potential problems with or without a degenerate boundary", *Eng. Anal. Boun. Elem.*, **24**, 671-684.
- Chen, J.T., Shen, W.C. and Wu, A.C. (2006), "Null-field integral equations for stress field around circular holes under antiplane shear", *Eng. Anal. Boun. Elem.*, **30**, 205-217.
- Chen, J.T. and Wu, A.C. (2007), "Null-field integral equation approach for the multi-inclusion problem under antiplane shears", *ASME J. Appl. Mech.*, **74**, 469-487.
- Chen, J.T., Lee, Y.T. and Chou, K.S. (2010), "Revisit of two classical elasticity problems by using the null-field integral equations", *J. Mech.*, **26**, 393-401.
- Chen, Y.Z. (1985), "A special boundary element formulation for multiple circular hole problems in an infinite plate", *Comput. Meth. Appl. Mech. Eng.*, **50**, 263-273.
- Chen, Y.Z. and Lin, X.Y. (2007), "Solution of periodic group circular hole problems by using the series expansion variational method", *Int. J. Numer. Meth. Eng.*, **69**, 1405-1422.
- Chen, Y.Z., Wang, Z.X. and Li, F.L. (2008), "Periodic group edge crack problem of half-plane in antiplane elasticity", *Commun. Numer. Meth. Eng.*, **24**, 833-840.
- Chen Y.Z., Wang, Z.X. and Lin, X.Y. (2009), "A new kernel in BIE and the exterior boundary value problem in plane elasticity", *Acta Mech.*, **206**, 207-224.
- Chen, Y.Z., Lin, X.Y. and Wang, Z.X. (2010), "Formulation of indirect BIEs in plane elasticity using single or double layer potentials and complex variable", *Eng. Anal. Boun. Elem.*, **34**, 337-351.
- Cheng, A.H.D. and Cheng, D.S. (2005), "Heritage and early history of the boundary element method", *Eng. Anal. Boun. Elem.*, **29**, 286-302.
- Cruse, T.A. (1969), "Numerical solutions in three-dimensional elastostatics", *Inter. J. Solids Struct.*, **5**, 1259-1274.
- Hong, H.K. and Chen, J.T. (1988), "Derivations of integral equations of elasticity", *J. Eng. Mech.* **114**, 1028-1044.
- Horii, H. and Nemat-Nassar, S. (1985), "Elastic fields of interacting inhomogeneities", *Int. J. Solids Struct.*, **21**,

- 731-745.
- Hromadka, T.V. (1987), *The Complex Variable Boundary Element Method in Engineering Analysis*, Springer, New York.
- Isida, M. and Igawa, H. (1991), "Analysis of a zig-zag array of circular holes in an infinite solid under uniaxial tension", *Int. J. Solids Struct.*, **27**, 849-864.
- Jaswon, M.A. and Symm, G.T. (1967), *Integral Equation Methods in Potential Theory and Elastostatics*, Academic Press, London.
- Linkov, A.M. (2002), *Boundary Integral Equations in Elasticity*, Kluwer, Dordrecht.
- Muskhelishvili, N.I. (1953), *Some Basic Problems of the Mathematical Theory of Elasticity*, Noordhoff, The Netherlands.
- Rizzo, F.J. (1967), "An integral equation approach to boundary value problems in classical elastostatics", *Quart. J. Appl. Math.*, **25**, 83-95.
- Ting, K., Chen, K.T. and Yang, W.S. (1999), "Stress analysis of the multiple circular holes with the rhombic array using alternating method", *Inter. J. Pres. Ves. Pip.*, **76**, 503-514.
- Tsukrov, I. and Kachanov, M. (1997), "Stress concentrations and microfracturing patterns in a brittle-elastic solid with interacting pores of diverse shapes", *Int. J. Solids Struct.*, **34**, 2887-2904.
- Wang, J.L., Crouch, S.L. and Mogilevskaya, S.G. (2003), "A complex boundary integral for multiple circular holes in an infinite plane", *Eng. Anal. Boun. Elem.*, **27**, 789-802.